

# Measurement Fractional Order Sallen-Key Filters

Ahmed Soltan, Ahmed G. Radwan, Ahmed M. Soliman

**Abstract**—This work aims to generalize the integer order Sallen-Key filters into the fractional-order domain. The analysis in the case of two different fractional-order elements introduced where the general transfer function becomes four terms which is unusual in the conventional case. In addition, the effect of the transfer function parameters on the filter poles and hence the stability is introduced and closed forms for the filter critical frequencies are driven. Finally, different examples for the fractional order Sallen-Key filter design are presented with circuit simulations using ADS where a great matching between the numerical and simulation results is obtained.

**Keywords**—Analog Filter, Low-Pass Filter, Fractance, Sallen-Key, Stability.

## I. INTRODUCTION

**F**ILTER design is one of the very few areas of electrical engineering for which a complete design theory exists. Whether passive or active, filters necessarily incorporate inductors and capacitors. Recently the scientists proved that the conventional inductor and capacitor are special cases from the more general so-called fractance device [1]. The impedance of this element in the complex frequency domain is given by  $Z(s) = k_o s^\alpha$ . Therefore, when  $\alpha = 1, -1$ , and  $0$ , this element represents an inductor, capacitor, and resistor respectively. Moreover, when  $\alpha = -2$ , it represents the well-known frequency-dependent negative resistor (FDNR) [2]. Then, the known circuit elements can be represented by this element by controlling on the fractional-order parameter  $\alpha$ . Generally, this element is an intermediate element whose properties are combinations between the known elements.

Sallen-Key filters are considered one of the most common and well-known filter families [3]. The conventional Sallen-Key family provides a second order filters by using two integer order capacitors and can be used to produce any of the special filters like the Butterworth filter response [4], [5]. Consequently, due to the importance of these filter family, this paper aims to convert the integer order Sallen-Key filters to the fractional domain and investigate the new fundamentals and properties in the presence of the two extra fractional-order parameters. So, this paper is organized as follows; Section II discusses the filter transfer function. Then, Section III determines a closed form for the filter critical frequencies. Section IV, presents different examples and circuit simulations

using advanced design system (ADS) for the proposed design procedure. Finally the conclusion section concludes the work.

## II. FILTER TRANSFER FUNCTION

Conventionally, the number of terms in the characteristic equation of any second order filters is three. However, fractional-order filters based on two fractional-elements can be divided into two types based on the number of terms in the characteristic equation either three or four terms. Many of the filter topologies have three terms in the denominator like the KHN and Tow-Tomas filters where their low pass transfer function is given by

$$T(s) = \frac{d}{s^{\alpha+\beta} + as^\alpha + c} \quad (1)$$

These Filters with transfer function similar to that of (1) have been discussed before in [6]–[8]. So, the aim of this work is to study the filters whose characteristic equation has four different terms as in the case of the Sallen-Key family where its low pass filter transfer function is given by

$$T(s) = \frac{d}{s^{\alpha+\beta} + as^\alpha + bs^\beta + c} \quad (2)$$

The characteristic equation for the low pass filter of the transfer function given in (2) is as follows:

$$D(j\omega, \alpha, \beta) = (\omega^{\alpha+\beta} \cos(0.5(\alpha + \beta)\pi) + a\omega^\alpha \cos(0.5\alpha\pi) + b\omega^\beta \cos(0.5\beta\pi) + c) + j(\omega^{\alpha+\beta} \sin(0.5(\alpha + \beta)\pi) + a\omega^\alpha \sin(0.5\alpha\pi) + b\omega^\beta \sin(0.5\beta\pi)) \quad (3)$$

Then, the magnitude squared of the characteristic equation  $|D(j\omega, \alpha, \beta)|^2$  can be obtained as

$$\begin{aligned} |D(j\omega, \alpha, \beta)|^2 = & \omega^{2(\alpha+\beta)} + b^2\omega^{2\beta} \\ & + a^2\omega^{2\alpha} + 2a\omega^{2\alpha+\beta} \cos(0.5\beta\pi) + 2b\omega^{\alpha+2\beta} \cos(0.5\alpha\pi) \\ & + (2ab \cos(0.5(\alpha - \beta)\pi) + 2c \cos(0.5(\alpha + \beta)\pi))\omega^{\alpha+\beta} \\ & + 2ca\omega^\alpha \cos(0.5\alpha\pi) + 2cb\omega^\beta \cos(0.5\beta\pi) + c^2 \end{aligned} \quad (4)$$

As a special case when  $\alpha = \beta$ , then (4) returns back to the special case presented in [6]. The stability of the filter represents one of the most important parameters of the filter design [9]. To study the filter stability, the effect of the transfer function parameters  $a$ , and  $c$  on the filter poles when  $(\alpha, \beta) = (1.6, 1.3)$  is presented in Fig. 1. When  $c = 10$  and at large negative values of  $a$  and  $b$ , the filter becomes unstable but as  $a$  or  $b$  increase the filter poles moves toward the stable region as shown in Fig. 1 (a). An interesting difference between the integer and the fractional-order cases is that the number of

Ahmed Soltan is with the Electronics and Communications Engineering Department, Fayoum University, Egypt (corresponding author to e-mail: asa03@fayoum.edu.eg).

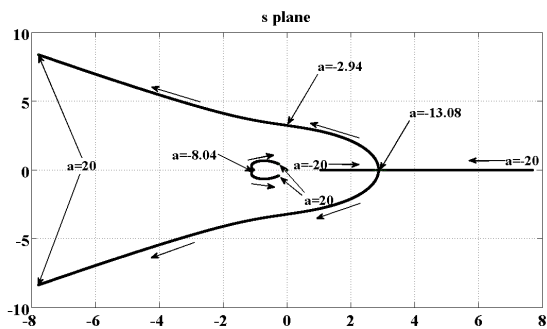
Ahmed G. Radwan is with the Engineering Mathematics Department, Faculty of Engineering, Cairo University, Egypt (e-mail: agradwan@iee.org).

Ahmed M. Soliman is with the Electronics and Communications Engineering Department, Faculty of Engineering, Cairo University, Egypt (e-mail: asoliman@iee.org).

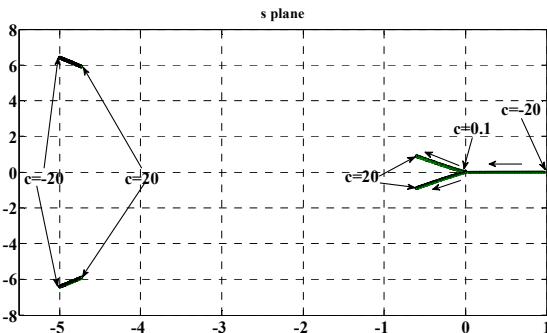
poles in the integer order system is fixed and depends only on the maximum order in the characteristic equation and doesn't affect by the other system parameter. However, the number of poles in the fractional-order systems becomes variable and dependent on the transfer function parameters besides the fractional orders  $\alpha$  and  $\beta$ .

TABLE I  
 SUMMARY OF THE STABILITY ANALYSIS AT  $(\alpha, \beta) = (1.6, 1.3)$

2-poles	3-poles	4-poles	Unstable	Stable
$(b, c) = (10, 10)$				
$a < -8.04$	-	$a \geq -8.04$	$a < -2.94$	$a \geq -2.94$
$(a, c) = (10, 10)$				
$b < -13.79$	-	$b \geq -13.79$	$b < -5.41$	$b \geq -5.41$
$(a, b) = (10, 10)$				
$c = 0$	$c < 0$	$c > 0$	$c < 0$	$c \geq 0$



(a)



(b)

Fig. 1 Change in the filter poles for  $(\alpha, \beta) = (1.6, 1.3)$  (a)  $b = c = 10$ , and (c)  $a = b = 10$

For example when  $(b, c, \alpha, \beta) = (10, 10, 1.6, 1.3)$ , the filter has two poles for  $a < -8.04$  and four poles for  $a \geq -8.04$ . This great advantage adds an extra degree of freedom to control the number of the filter poles without affecting the system order. The filter starts to be stable for  $a \geq -2.94$ , this means the filter can be designed for negative values of  $a$  or  $b$  and remains stable which adds an extra degree of freedom in the filter design. Similar analysis can be made for the parameters  $b$  and  $c$  of the filter as shown in Fig. 1 (b). A summary of the stability analysis and the effect of the parameters  $a, b$ , and  $c$  on the poles movement and the number of poles at  $(\alpha, \beta) = (1.6, 1.3)$  are tabulated in Table I.

### III. CRITICAL FREQUENCIES

The following subsections studies the general formulas of the three critical frequencies of interest for the filter design  $\{\omega_m, \omega_h, \omega_{rp}\}$  [7].

#### A. The Maximum and Minimum Frequencies ( $\omega_m$ )

The maximum and minimum frequencies points are considered very important because they determine the ripples in the pass-band. Hence, these frequency points can be used as a measure for the attenuation in the filter pass-band. These frequency points are obtained by solving the equation  $(d|T(j\omega, \alpha, \beta)|/d\omega)_{\omega=\omega_m} = 0$ . Consequently, the maximum and minimum frequency points can be obtained by:

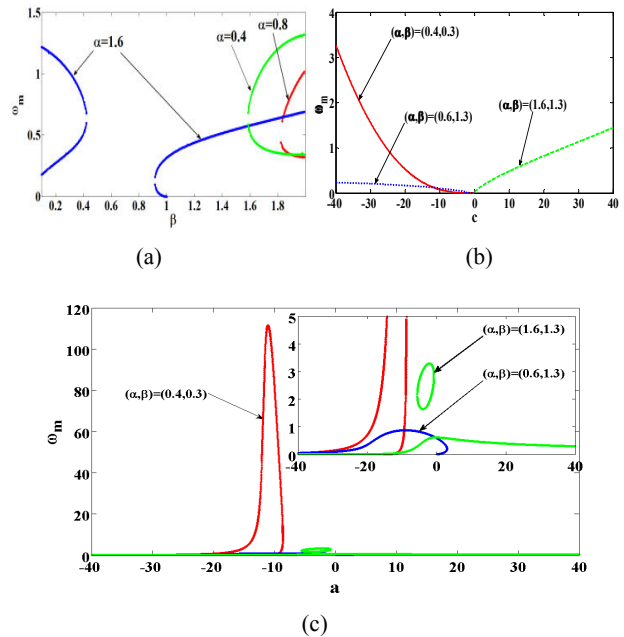


Fig. 2 (a) Effect of  $\beta$  on  $\omega_m$  at different values of  $\alpha$  for  $a = b = c = 10$ , (b) Change in  $\omega_m$  with respect to  $c$  at different values of  $\alpha$  and  $\beta$  for  $a = b = 10$ , (c) Effect of  $a$  on  $\omega_m$  at different values of  $\alpha$  and  $\beta$  for  $b = c = 10$

$$\omega_m^{2(\alpha+\beta)} + \frac{\beta b^2}{\alpha+\beta} \omega_m^{2\beta} + \frac{a a^2}{\alpha+\beta} \omega_m^{2\alpha} + \frac{(2\alpha+\beta)a \cos(\frac{\beta\pi}{2})}{\alpha+\beta} \omega_m^{2\alpha+\beta} + \frac{(2\beta+\alpha)b \cos(\frac{\alpha\pi}{2})}{\alpha+\beta} \omega_m^{2\beta+\alpha} + \frac{a a c \cos(\frac{\alpha\pi}{2})}{\alpha+\beta} \omega_m^\alpha + \left( a b \cos\left(\frac{(\alpha-\beta)\pi}{2}\right) + c \cos\left(\frac{(\alpha+\beta)\pi}{2}\right) \right) \omega_m^{\alpha+\beta} + \frac{\beta b c}{\alpha+\beta} \omega_m^\beta = 0 \quad (5)$$

From (5), the maximum and minimum frequency points depend on the fractional orders  $\alpha$  and  $\beta$  besides the transfer function parameters  $a, b$ , and  $c$ . The effect of these design parameters on  $\omega_m$  is depicted in Fig. 2 at different conditions. The solution of (5) can produce no, one, two or three solutions depending on the value of the transfer function parameters as shown in Figs. 2 (a)-(c). To demonstrate these different cases of the solution of (5), the frequency response of (2) is presented in Fig. 3 at different conditions. The frequency response of Fig. 3 (a) has three values of  $\omega_m$  at the condition  $(a, b, c, \alpha, \beta) = (-2, 10, 10, 1.6, 1.3)$  which confirms the result presented in Fig.

2 (c). Also, the frequency response of Figs. 3 (b), (c) has two and one value of  $\omega_m$  respectively at conditions obtained from Fig. 2 (a). The frequency response for the case of no valid solution of  $\omega_m$  is presented in Fig. 3 (d). Due to the symmetry of the transfer function, the effect of  $\alpha$  on  $\omega_m$  is the same as that of  $\beta$ . As shown in Fig. 2 (c), the solution of (5) with respect to  $a$  results one solution or three solutions. This means that, for the case of three values of  $\omega_m$ , the filter is suffering from damping in the pass-band of the filter as shown in the

frequency response of Fig. 3 (a). In addition, the filter has a valid solution for  $\omega_m$  for negative values of  $a$ , this means that the filter can be designed for negative impedance which increases the design degree of freedom.

Also, the effect of  $b$  on  $\omega_m$  is the same as the effect of  $a$  because of the symmetry of the transfer function. Finally, the effect of  $c$  on  $\omega_m$  is presented in Fig. 2 (b) which depicts that the filter can have a solution also for negative values of  $c$  which increases the design flexibility.

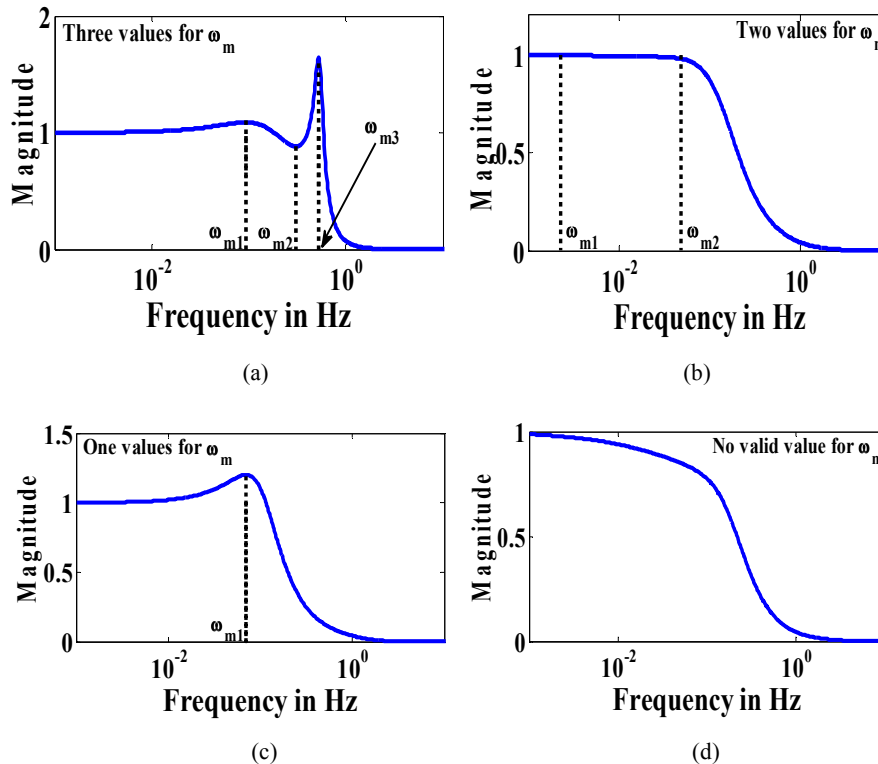


Fig. 3 Magnitude response of the fractional Sallen-Key filter when (a)  $(a, b, c, \alpha, \beta) = (-2, 10, 10, 1.6, 1.3)$ , (b)  $(a, b, c, \alpha, \beta) = (10, 10, 10, 1.6, 0.9)$ , (c)  $(a, b, c, \alpha, \beta) = (10, 10, 10, 1.6, 1.3)$ , (d)  $(a, b, c, \alpha, \beta) = (10, 10, 10, 1.6, 0.7)$

### B. The Half Power Frequency

The half power frequency ( $\omega_h$ ) point is used to calculate the filter bandwidth. Then, the value of  $\omega_h$  is calculated from the relation  $|T(j\omega_h)| = (1/\sqrt{2})|T(j\omega_{pasband})|$ . Hence from (3), the value of  $\omega_h$  can be calculated from the following relation:

$$\begin{aligned}
 &\omega_h^{2(\alpha+\beta)} + b^2\omega_h^{2\beta} + a^2\omega_h^{2\alpha} \\
 &+ 2a\omega_h^{2\alpha+\beta} \cos(0.5\beta\pi) + 2b\omega_h^{\alpha+2\beta} \cos(0.5\alpha\pi) \\
 &+ (2ab \cos(0.5(\alpha - \beta)\pi) + 2c \cos(0.5(\alpha + \beta)\pi))\omega_h^{\alpha+\beta} \\
 &+ 2ca\omega_h^\alpha \cos(0.5\alpha\pi) + 2cb\omega_h^\beta \cos(0.5\beta\pi) - c^2 = 0 \quad (6)
 \end{aligned}$$

Consequently, the half power frequency depends on the value of  $a, b, c, \alpha$  and  $\beta$ , which adds an extra degree of design freedom. It is clear from Fig. 4 that the solution of (6) has at least one solution for  $\omega_h$  which is expected, but some of these values lie in the unstable region. In addition, near the unstable region the filter is suffering from a very strong damping where

more than one solution of (6) exists as shown in Fig. 4 (a). When  $a = b = 10$  and for a wide range of  $c$ , the filter has a single  $\omega_h$  as shown in Fig. 4 (b). As shown in Fig. 4 (c), the filter can be designed for negative values of  $a$  if the filter is stable under these conditions which add extra degree of freedom. Due to the symmetry of the filter transfer function, the effect of  $\alpha$  and  $b$  on  $\omega_h$  is the same as that of  $\beta$  and  $a$  respectively.

### C. The Right Phase Frequency

The right phase frequency ( $\omega_{rp}$ ) is the frequency where its phase response  $\angle T(j\omega_{rp}) = \pm \frac{\pi}{2}$  and the transfer function  $T(s)$  becomes pure imaginary at  $\omega_{rp}$ . Hence, the  $\omega_{rp}$  can be calculated as follows:

$$\omega_{rp}^{\alpha+\beta} \cos(0.5(\alpha + \beta)\pi) + a\omega_{rp}^\alpha \cos(0.5\alpha\pi) + b\omega_{rp}^\beta \cos(0.5\beta\pi) + c = 0 \quad (7)$$

For the traditional case ( $\alpha = \beta = 1$ ), the value of the right phase frequency is given by  $\omega_{rp} = \sqrt{c}$  [6]. From (7), the right phase frequency ( $\omega_{rp}$ ) is dependent on the fractional orders  $\alpha$ , and  $\beta$  besides the transfer function parameters  $a, b$ , and  $c$ . As shown in Fig. 5, the effect of the fractional orders  $\alpha$  and  $\beta$  is symmetric. So, the filter can be designed for a different values of  $\omega_h$  and  $\omega_{rp}$ .

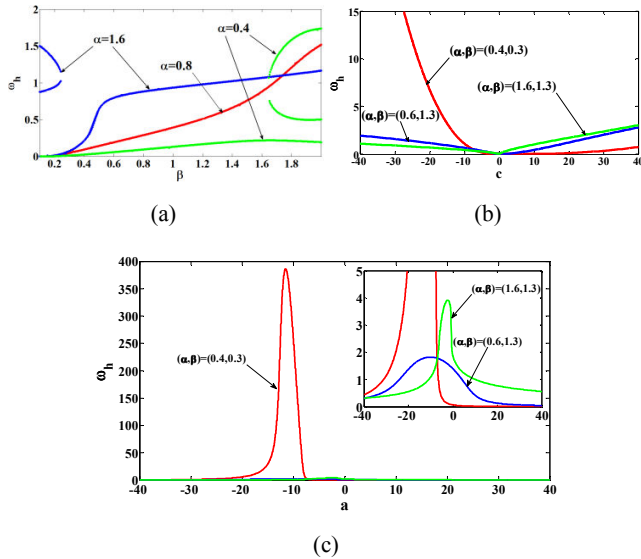


Fig. 4 (a) Change in  $\omega_h$  with respect to  $\beta$  at different values of  $\alpha$  for  $a = b = c = 10$ , (b) Effect of  $c$  on  $\omega_h$  at different values of  $\alpha$  and  $\beta$  for  $a = b = 10$ , and (c) Change in  $\omega_h$  with respect to  $a$  at different values of  $\alpha$  and  $\beta$  for  $b = c = 10$

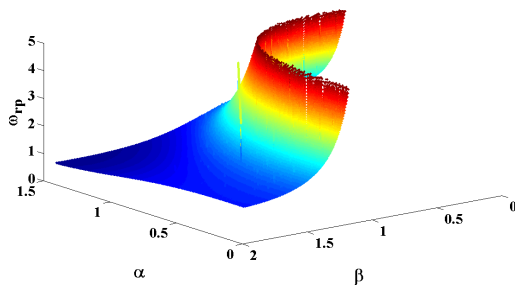


Fig. 5 Change in  $\omega_{rp}$  with respect to  $\alpha$  and  $\beta$  for  $a = b = c = 10$

It is clear from Fig. 5 that the change in  $\omega_{rp}$  is large when  $\alpha$  and  $\beta < 1$ . On the other hand, the change is negligible for  $\alpha$  and  $\beta > 1$ .

#### IV. SIMULATION RESULTS

The effect of the fractional orders  $\alpha$  and  $\beta$  on the filter response is demonstrated in the 3D plot for (1) given in Fig. 6 at  $\omega_h = 1\text{rad/sec}$ . It is interesting to note here that, as the value of  $\alpha$  increase, the filter bandwidth decrease for the same parameters. Yet, a notch appears for large values of  $\alpha$  which adds an independent control on the filter bandwidth and increases the design degree of freedom. Finally, the effect of  $\beta$  is the same as the effect of  $\alpha$  on the filter frequency response because of the symmetry of the transfer function of (1).

During the last ten years, several promising trials have been introduced for the realizations of the fractional element and based on different techniques such as chemical reactions [10], fractal shapes [11], and graphene material [12]. Moreover, many finite circuit approximations were suggested to model the fractional order elements [13], [14] such as the subplot of Fig. 7 (a). The fractional order Sallen-Key filter after replacing the integer order capacitors with two fractional order elements of orders  $\alpha$  and  $\beta$  is presented in Fig. 7 (a). The fractional order filter transfer function can be written as follows:

$$\frac{V_{out}}{V_{in}} = \frac{\frac{1}{R_1 R_2 C_1 C_2}}{s^{\alpha+\beta} + \frac{1-R_4/R_3}{R_2 C_2} s^\alpha + \left(\frac{1}{R_2 C_1} + \frac{1}{R_1 C_1}\right) s^\beta + \frac{1}{R_1 R_2 C_1 C_2}} \quad (8)$$

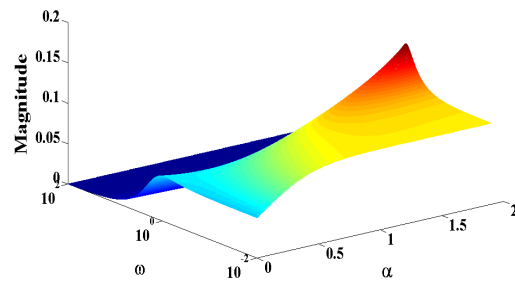


Fig. 6 Effect of  $\alpha$  on the frequency response of the filter at  $\beta = 1.3$  and for  $a = b = c = 10$  and  $\omega_h = 1\text{rad/sec}$

Consequently, to design the SK filter for a specific bandwidth ( $\omega_h$ ), then (6) can be rearranged to calculate the value of the missing design parameter for a given  $\omega_h$ . The same steps can be followed to design the filter for a specific  $\omega_m$  or  $\omega_{rp}$ . In addition, the filter can be designed for specific values of three critical frequency points  $\omega_m$ ,  $\omega_h$ , and  $\omega_{rp}$  by solving (5), (6), and (7) to calculate the transfer function parameters. Besides, there are remaining two parameters as a design degree of freedom and to control the filter stability, and then the circuit components using (8) or the relation summarized in Table II can be achieved.

By using the previous described procedure on the Sallen-key filter of Fig. 7 (a), the circuit simulation using ADS for the fractional order Sallen-Key filter is depicted in Fig. 7 (b) at  $\omega_h = 10\text{rad/sec}$  with two different orders.

TABLE II  
 RELATION BETWEEN THE CIRCUIT COMPONENTS AND THE TRANSFER FUNCTION PARAMETERS

Parameter	Relation
$a$	$(1 - R_4/R_3)/R_2 C_2$
$b$	$(1/C_1)(1/R_1 + 1/R_2)$
$c$	$1/(C_1 C_2 R_1 R_2)$
$d$	$1/(C_1 C_2 R_1 R_2)$

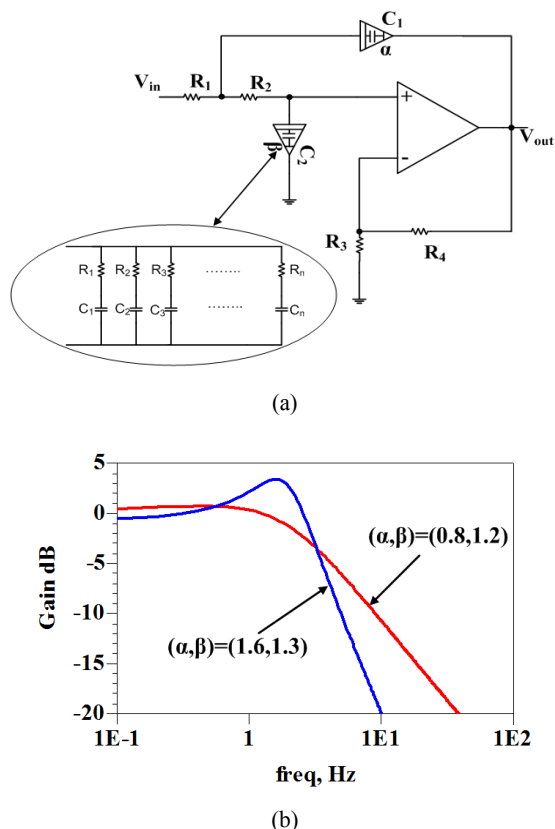


Fig. 7 (a) Fractional order Sallen-Key filter, (b) circuit simulation of the filter at  $\omega_h = 10\text{rad/sec}$  for different orders

The slopes of both simulations are different as shown in Fig. 7 (b) where the slope equals  $(\alpha + \beta)20\text{dB/decade}$  and for two different cases  $(R_1, R_2, C_1, C_2, R_4/R_3, \alpha, \beta) = (8.44\text{k}\Omega, 86.8\text{k}\Omega, 10\mu, 10\mu, 12.8, 1.6, 1.3)$  and  $(7.11\text{k}\Omega, 30.63\text{k}\Omega, 20\mu, 50\text{n}, 0.8836, 0.8, 1.2)$ . Finally, frequency scaling can be used to obtain the required  $\omega_h$  for the demonstrated fractional orders [8].

## V. CONCLUSION

A design procedure for designing fractional order Sallen-Key filter with different fractional-orders was proposed here. More design flexibility is obtained due to the large number of the transfer function parameters. So, the design degree of freedom is increase in the fractional-order domain. The effect of the transfer function parameters and the fractional orders on the filter poles and stability are discussed. Besides, a closed form for the critical frequency points is introduced. Circuit simulation for the practical Sallen-Key filter is also presented.

## REFERENCES

- [1] B. T. Krishna, "Studies on fractional order differentiators and integrators: A survey," *Signal Processing*, vol. 91, no. 3, pp. 386-426, 2011.
- [2] A. G. Radwan, A. M. Soliman, and A. S. Elwakil, "First-order filters generalized to the fractional domain," *Journal of Circuits, Systems, and Computers*, vol. 17, no. 01, pp. 55-66, 2008.
- [3] R.P. Sallen and E.L. Key, "A practical method of designing RC active filters," *Circuit Theory, IRE Transactions on*, vol. 2, no. 1, pp. 74-85, 1955.

- [4] A. Soltan, A. G. Radwan, and A.M. Soliman, "Butterworth passive filter in the fractional-order," in *Microelectronics (ICM), 2011 International Conference on*, 2011, pp. 1-5.
- [5] A. S. Ali, A. G. Radwan, and A. M. Soliman, "Fractional Order Butterworth Filter: Active and Passive Realizations", *Emerging and Selected Topics in Circuits and Systems, IEEE Journal on*, vol.3, no.3, pp.346 - 354, 2013
- [6] A. G. Radwan, A. S. Elwakil, and A. M. Soliman, "On the generalization of second-order filters to the fractional-order domain," *Journal of Circuits, Systems, and Computers*, vol. 18, no. 02, pp. 361-386, 2009.
- [7] A. Soltan, A. G. Radwan, and A. M. Soliman, "Fractional order filter with two fractional elements of dependant orders," *Microelectronics Journal*, vol. 43, pp. 818 – 827, 2012.
- [8] A. Soltan, A. G. Radwan, A. M. Soliman, "CCII based fractional filters of different orders", *J Adv Res*, DOI: 10.1016/j.jare. 2013.01.007, 2013
- [9] A.G. Radwan, A.M. Soliman, A.S. Elwakil, and A. Sedeek, "On the stability of linear systems with fractional-order elements," *Chaos, Solitons & Fractals*, vol. 40, no. 5, pp. 2317-2328, 2009.
- [10] K. Biswas, S. Sen, and P. K. Dutta, "A constant phase element sensor for monitoring microbial growth," *Sensors and Actuators B: Chemical*, vol. 119, no. 1, pp. 186-191, 2006.
- [11] T. C. Haba, G. Ablart, T. Camps, and F. Olivie, "Influence of the electrical parameters on the input impedance of a fractal structure realised on silicon," *Chaos, Solitons & Fractals*, vol. 24, no. 2, pp. 479-490, 2005.
- [12] A. M. Elshurafa, M. N. Almadhoun, K. N. Salama, and H. N. Alshareef, "Microscale electrostatic fractional capacitors using reduced graphene oxide percolated polymer composites," *Applied Physics Letters*, vol. 102, no. 23, p. 232901, 2013.
- [13] M. Nakagawa and K. Sorimachi, "Basic characteristics of a fractance device," *IEICE Transactions on Fundamentals of Electronics, Communications and Computer Sciences*, vol. 75, no. 12, pp. 1814-1819, 1992.
- [14] S. Michio, Y. Hirano, Y. F. Miura, and K. Saito, "Simulation of fractal immittance by analog circuits: an approach to the optimized circuits," *IEICE Transactions on Fundamentals of Electronics, Communications and Computer Sciences*, vol. 82, no. 8, pp. 1627-1635, 1999.